

# Monomer-Dimer Mixture on a Honeycomb Lattice

Hiromi Otsuka

*Department of Physics, Tokyo Metropolitan University, Tokyo 192-0397, Japan*

(Dated: October 18, 2018)

We study a monomer-dimer mixture defined on a honeycomb lattice as a toy model for the spin ice system in a magnetic field. In a low-doping region of monomers, the effective description of this system is given by the dual sine-Gordon model. In intermediate- and strong-doping regions, the Potts lattice gas theory can be employed. Synthesizing these results, we construct a renormalization-group flow diagram, which includes the stable and unstable fixed points corresponding to  $\mathcal{M}_5$  and  $\mathcal{M}_6$  in the minimal models of the conformal field theory. We perform numerical transfer-matrix calculations to determine a global phase diagram and also to proffer evidence to check our prediction.

PACS numbers: 75.40.Cx, 05.50.+q, 05.70.Jk

An introductory study of dimer degrees of freedom for condensed matter physics was carried out long time ago. In a paper by Fowler and Rushbrooke in 1937, the dimer represented a diatomic molecule adsorbed on a crystal surface [1]. Later, the statistical mechanics of dimers was studied by Kasteleyn [2] and Temperley and Fisher [3]. These pioneering works have provided exact solutions of two-dimensional models under certain conditions. Since then, dimer models have gathered increasing attention.

The correspondence between dimer models and real substances seems to fall into two categories. First, like for the case of diatomic molecules, the correspondence originates in the shape of the elements. For example, recently a network system made of rodlike molecules on a substrate was measured by using scanning tunneling microscopy [4]. It was argued that, because of the shape of the molecules, a honeycomb-lattice dimer model can be employed to reproduce properties of the network [5]. Second, the correspondence can originate in interactions between elements. Spin configurations in the ground state of a triangular-lattice antiferromagnetic Ising model can be related to those of dimers on a honeycomb lattice [6]. In this case, dimer degrees of freedom emerge on a different lattice and represent unsatisfied bonds.

In this work, we investigate a dimer-based model which can be related, in the latter sense, to the spin ice in a magnetic field. To describe their relevance, we begin by summarizing related researches. The rare-earth titanates such as  $R_2\text{Ti}_2\text{O}_7$  ( $R = \text{Ho}, \text{Dy}$ ) are known as the Ising pyrochlore magnets (IPM) [7], where each  $R^{3+}$  behaves as an Ising spin along a local axis pointing in the center of a tetrahedron. In the low temperature, due to the magnetic couplings [8], six states, satisfying the so-called 2-in-2-out condition (also known as the ice rule), are permitted for each tetrahedron. When a magnetic field is applied along its [111] direction, a plateau is observed at  $\frac{2}{3}$  of the saturation magnetization [9, 10]. This incompressible state is called the kagome ice. For a kagome layer sandwiched between two triangular layers, only three states are permitted for each tetrahedron pointing in the [111] ( $[\bar{1}\bar{1}\bar{1}]$ ) direction since spins on the triangular layers are polar-

ized. Then, the mapping from the spin configuration on the kagome layer to the dimer configuration on the honeycomb lattice is possible, which enables us to exactly enumerate the residual entropy [11].

While the magnetic field causes a dimensional reduction, it also induces low-energy excitations that lead to breakings of the ice rule: For each tetrahedron pointing in the [111] ( $[\bar{1}\bar{1}\bar{1}]$ ) direction, a state that minimizes the Zeeman energy takes the 3-in-1-out (1-in-3-out) configuration. This state can be viewed as a magnetic monopole (antimonopole) in the solid [12–15]. Specific heat measurement revealed that the temperature dependence of the monopole density obeys the Arrhenius law with an energy scale controlled by the magnetic field [14]. So, monopole excitation effects become significant at least around the phase boundary between the kagome ice and a saturated state [12, 15]. We note that since monopole-antimonopole pair creations and annihilations are only permitted, it follows naturally to introduce monomers in the dimer model to describe them.

Motivated by the research advances on IPM, we consider a monomer-dimer mixture (MDM) on a honeycomb lattice  $\Lambda_H$ . When we write the dimer occupation number on the kagome lattice  $\Lambda_K$  (the medial lattice of  $\Lambda_H$ ) as  $n_l = 0, 1$ , then a reduced Hamiltonian is given by

$$\beta H = u \sum_{\rho=a,b,c} \sum_{\langle l,m \rangle \in \Lambda_K^\rho} n_l n_m - \mu \sum_{l \in \Lambda_K} n_l \quad (1)$$

( $\Lambda_K^{a,b,c}$ , three sublattices of  $\Lambda_K$ ). The first term represents the interaction between two neighboring dimers and the second term signifies the chemical potential that controls the density of dimers (and thus monomers). In addition, we impose the hard-core constraint,  $\forall j \in \Lambda_H$ ,  $\sum_{l \in \{l(j)\}} n_l = 0, 1$ , where  $\{l(j)\}$  denotes three sites around  $j$ . For the compounds under consideration, the long-range dipole interaction is expected to be large [8]. While the so-called projective equivalence explains their spin-ice behaviors [16], the long-range nature may become important with breaking the ice rule. Here, we have employed the oversimplified model with the short-range interaction because we focus on universal proper-

ties stemming from a competition between the interaction and the monomer doping effects, which could shed some light on the understanding of, for instance, the properties of monopoles in the Kagome ice.

The MDM system on the square lattice was discussed by several authors [17, 18], where an effective theory for long-distance behaviors plays an important role. We take a similar approach; however our analysis predicts the emergence of criticalities not observed in the square lattice case. Let us start with the dimer covering case without the interaction ( $u = 0$ ,  $\mu = \infty$ ). Its critical behaviors are described by a two-dimensional sine-Gordon Lagrangian density  $\mathcal{L}_0 = \mathcal{L}_G + \mathcal{L}_\varphi$  with

$$\mathcal{L}_G = \frac{K}{2\pi} (\nabla\varphi)^2, \quad \mathcal{L}_\varphi = \frac{y_\varphi}{2\pi\alpha^2} : \cos 3\sqrt{2}\varphi : . \quad (2)$$

We have denoted the coarse-grained height field as  $\varphi(\mathbf{x})$ , which satisfies the periodicity condition  $\sqrt{2}\varphi = \sqrt{2}\varphi + 2\pi N$  with  $N \in \mathbb{Z}$  ( $\alpha$ , a short distance cutoff) [17, 19]. Since the Gaussian coupling  $K$  equals  $\frac{1}{2}$ , the nonlinear term  $\mathcal{L}_\varphi$  that represents the discreteness in the original height field is irrelevant ( $y_\varphi$ , a negative constant).

Next, we consider a modification of  $\mathcal{L}_0$  that is brought about by the nearest-neighbor interaction. Jacobsen and Alet discussed the same effect in a somewhat different context [5] and concluded that, like the square-lattice case, it is devoted to a renormalization of the Gaussian coupling [18, 20]. Thus, we can write  $K(u) \simeq \frac{1}{2} + c_1 u$  ( $c_1$ , a negative constant). On the other hand, a monomer on, say, the A (B) sublattice of  $\Lambda_H$  corresponds to a defect with a positive (negative) charge. In the sine-Gordon language, using the disorder field  $\vartheta$  dual to  $\varphi$ , we can express monomers as  $e^{\pm i\sqrt{2}\vartheta}$ . Consequently, at least in the low-doping region, a dual sine-Gordon model  $\mathcal{L} = \mathcal{L}_G(u) + \mathcal{L}_\varphi + \mathcal{L}_\vartheta$  describes the MDM system, where

$$\mathcal{L}_\vartheta = \frac{y_\vartheta}{2\pi\alpha^2} : \cos \sqrt{2}\vartheta : \quad (3)$$

and a fugacity of monomers  $y_\vartheta \propto e^{-\mu/2}$ . To proceed further, we clarify a renormalization-group (RG) flow in the attractive region  $u \leq 0$ . Since the dimensions of  $\cos 3\sqrt{2}\varphi$  and  $\cos \sqrt{2}\vartheta$  are  $9/2K$  and  $K/2$ , respectively, the Gaussian fixed line is realized for  $\frac{1}{2} \leq K \leq \frac{9}{4}$  in the dimer covering case, whereas it is unstable against the doping. We sketch the flow in Fig. 1 (see the red region), where  $(w, z) = (e^{-u}, e^{-\mu/2})$ . The open circle on the  $w$  axis denotes the end point  $K = \frac{9}{4}$ , where  $\mathcal{L}_\varphi$  becomes marginal and brings about the Berezinskii-Kosterlitz-Thouless (BKT) transition to the 3-fold degenerate columnar ordered state, as shown by the flow to the filled triangle. Meanwhile the relevant  $\mathcal{L}_\vartheta$  leads to the disordered phase (see the flow to the filled circle).  $\mathcal{L}_\varphi$  and  $\mathcal{L}_\vartheta$  are mutually non-local, so intrinsically they are in competition. If both of them are relevant, it becomes obvious as a flow to an infrared (IR) fixed point. Since

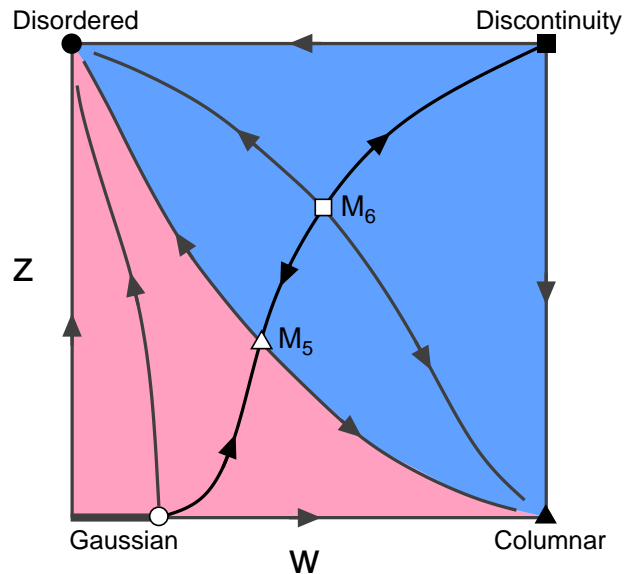


FIG. 1: (Color online) A rough sketch of the RG flow diagram. The open circle denotes the end point of the Gaussian fixed line on the  $w$  axis; the marks for fixed points are given with explanations. The sine-Gordon theory (the Potts lattice gas theory) is varied in the red (blue) region.

this fixed point describes the transition to the 3-fold degenerate ordered state, it may be of the 3-state Potts universality class. Consequently, we can expect a massless RG flow from the ultraviolet (UV) fixed point with the central charge  $c = 1$  (the open circle) to the IR fixed point with  $c = \frac{4}{5}$  (the open triangle) [21]. Indeed,  $\mathcal{L}$  is an effective theory for the 3-state Potts model, and, under the self-dual condition, this flow has been explicitly obtained and understood as a renormalization of the  $\mathbb{Z}_3$  neutral  $X$  operator, with dimension  $x_X = \frac{14}{5}$ , to the IR fixed point [21]. Although  $\mathcal{L}$  is not self-dual around the open circle, we suppose that the same RG flow should be observed at least around the open triangle. We provide numerical evidence for this assumption below.

For the exploration of intermediate- and strong-doping regions, let us focus on the role of the  $X$  operator. Writing the minimal model series of the conformal field theory with  $c = 1 - 6/p(p+1)$  as  $\mathcal{M}_p$  and a primary field at the position  $(r, s)$  of the conformal grid as  $\phi_{r,s}^{(p)}$ , then  $X = \phi_{3,1}^{(5)}$ , i.e., the *leading irrelevant* operator on  $\mathcal{M}_5$ . Zamolodchikov [22] and Ludwig and Cardy [23] discussed the deformation of  $\mathcal{M}_p$  by the *least relevant* operator  $\phi_{1,3}^{(p)}$  and concluded that there exists a RG flow connecting minimal models as

$$\text{UV} : \mathcal{M}_p, \phi_{1,3}^{(p)} \longrightarrow \text{IR} : \mathcal{M}_{p-1}, \phi_{3,1}^{(p-1)}, \quad (4)$$

where a UV-IR operator transmutation is also given. By taking these into account, it is plausible that another UV fixed point exists and that a RG flow connects  $\mathcal{M}_6$  (the open square) and  $\mathcal{M}_5$  (the open triangle), as given in Fig.

1. In the opposite direction, the renormalization always amplifies a deviation from  $\mathcal{M}_6$ , so the coupling of  $\phi_{1,3}^{(6)}$  flows to a strong-coupling fixed point (the filled square). It may be a discontinuity one, and thus the transition is of first order in the strong-doping region.

The emergence of the new critical fixed point  $\mathcal{M}_6$  with  $c = \frac{6}{7}$  is key to understanding the MDM system. We take a look at the following UV-IR operator correspondence and characterize it [23].

$$\text{UV} : \phi_{1,3}^{(6)}, \phi_{5,5}^{(6)}, \phi_{3,3}^{(6)} \longrightarrow \text{IR} : \phi_{3,1}^{(5)}, \phi_{2,1}^{(5)}, \phi_{3,3}^{(5)}. \quad (5)$$

The latter two of the three IR operators correspond to the energy density ( $\varepsilon$ ) and the  $\mathbb{Z}_3$  spin ( $\sigma$ ) of the 3-state Potts model, respectively. Thus,  $\phi_{1,2}^{(6)}$  ( $= \phi_{5,5}^{(6)}$ ) as well as  $\phi_{1,3}^{(6)}$  is  $\mathbb{Z}_3$  neutral, and represents a thermal operator in the Lagrangian. Since, using the Kac formula, dimensions of UV operators are given as  $x_{1,3}^{(6)} = \frac{10}{7}$ ,  $x_{1,2}^{(6)} = \frac{4}{7}$ , and  $x_{3,3}^{(6)} = \frac{2}{21}$ ,  $\phi_{1,3}^{(6)}$  and  $\phi_{1,2}^{(6)}$  are both relevant and provide the flow around the open square in Fig. 1. In the literature, one can find a model that exhibits the same RG flow given in the blue region of Fig. 1. Nienhuis discussed the  $q$ -state Potts lattice gas model on a square lattice [24], where the leading and next-leading thermal exponents were obtained on both the critical and tricritical points. Indeed, for  $q = 3$ , those on the latter are  $y_1 = \frac{4}{7}$  and  $y_2 = \frac{12}{7}$ , which agree with the dimensions  $x_{1,3}^{(6)}$  and  $x_{1,2}^{(6)}$ . Therefore, the MDM system in the intermediate- and strong-doping regions can be viewed as the 3-state Potts lattice gas, where monomers and dimers play roles of the vacancies and the  $\mathbb{Z}_3$  spins, respectively.

Obviously, the 3-fold axis symmetry in  $\Lambda_H$  plays a decisive role in determining  $\mathcal{L}_\varphi$  and mapping to the Potts lattice gas with  $q = 3$ . In contrast, for the MDM on the square lattice [17, 18], due to the 4-fold axis symmetry, the sine-Gordon theory with a potential  $\cos 4\sqrt{2}\varphi$  and a 4-state Potts lattice gas theory are relevant in the weak- and strong-doping regions, respectively. So, instead of crossovers of criticalities, we observe a fixed line that terminates by the first-order phase transition line.

Now, we explain numerical calculations and results to check our prediction. We have focused on a structure of the phase diagram and the universality classes of phase transitions. We first summarize our results on the phase diagram in Fig. 2. We quote the BKT point of [5],  $w_{\text{BKT}} \simeq 1/0.635$ , which is indicated by the open circle on the  $w$  axis. The curve for open triangles (filled squares) denotes the second-order (first-order) phase transition boundary  $z_2(w)$  [ $z_1(w)$ ] between the ordered and disordered phases. The open square represents the tricritical point. For their enumerations, we have performed numerical transfer-matrix calculations of Eq. (1) on  $\Lambda_H$  with  $L \times \infty$  cylinder geometry [ $L$ , the circumference of the cylinder in units of the length between two parallel bonds, is given in multiples of 3 because the columnar

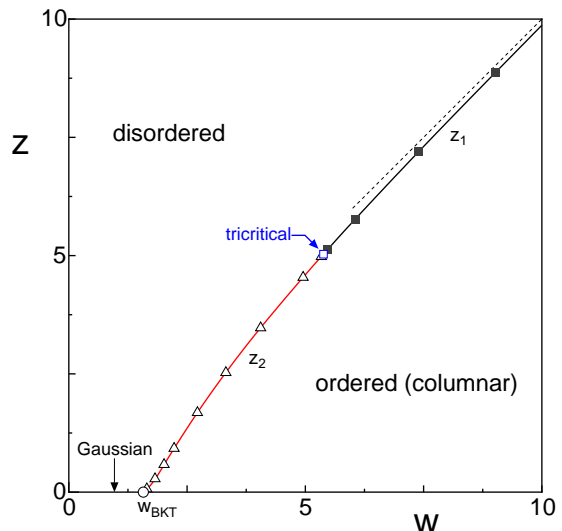


FIG. 2: (Color online) The global phase diagram. Open triangles (filled squares) represent the second-order (first-order) phase transition points; the open square denotes the tricritical point. The dotted line gives the asymptotic form  $z = w$ .

state is expected]. We note that, with the monomer doping, the row-to-row transfer matrix  $\mathbf{T}(L)$  becomes less sparse. Thus, the accessible system size is strongly limited to a small number, e.g.,  $L \leq 12$  in our calculations.

To determine the second-order phase transition points, we have performed phenomenological RG (PRG) calculations. Writing the eigenvalues of  $\mathbf{T}(L)$  as  $\lambda_i(L)$  and their logarithms as  $E_i(L) = -\ln |\lambda_i(L)|$  ( $i$  specifies an excitation), then the conformal invariance provides the direct expressions of  $c$  and  $x_i$  in the critical systems as  $E_g(L) \simeq Lf - \pi c/6L\zeta$  and  $\Delta E_i(L) \simeq 2\pi x_i/L\zeta$  [25, 26].  $E_g(L)$ ,  $\Delta E_i(L)$  [ $= E_i(L) - E_g(L)$ ],  $\zeta$  ( $= \sqrt{3}/2$ ), and  $f$  correspond to the ground-state energy, an excitation gap, the geometric factor, and the free-energy density, respectively.  $E_g$  is found in the zero momentum sector ( $k = 0$ ). Also,  $E_i$  is in a sector specified by its symmetry property. In the PRG calculation, we have employed the lowest excitation, corresponding to  $\sigma$ , with  $k = 2\pi/3$ . We then numerically solve the condition  $L\Delta E_\sigma(L) = L'\Delta E_\sigma(L')$  with respect to  $z$  for given values of  $w$ . We have extrapolated finite-size estimates of  $L = 6, 9$ , and  $12$  to the thermodynamic limit based on an assumption of the leading  $O(L^{-2})$  correction [27]. Then, we find that the curve  $z_2(w)$  continues smoothly to the open circle  $w_{\text{BKT}}$ , which exhibits a consistency with the previous result [5].

To check the universality class, we evaluate  $c$  and  $x_\sigma$  along  $z_2(w)$ . Plotted in Figs. 3(a) and 3(b) are the extrapolated results [28]. Although we cannot extract reliable data around  $w_{\text{BKT}}$  due to the smallness of the system size, we can find evidence to support the 3-state Potts universality  $c = \frac{4}{5}$  and  $x_\sigma = \frac{2}{15}$  down to  $u \simeq -1.5$ . Also, Fig. 3(c) provides a finite-size scaling plot of the gap  $\Delta E_\sigma(L) = L^{-1}\Psi\{[z - z_2(w)]L^{\frac{1}{\nu}}\}$  at  $u = -1$ . Since

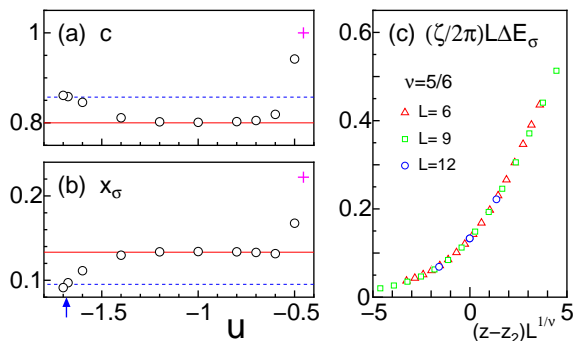


FIG. 3: (Color online) The estimations (open circles) of (a)  $c$  and (b)  $x_\sigma$  along  $z_2(w)$ . Solid and dotted lines denote theoretical values for  $\mathcal{M}_5$  and  $\mathcal{M}_6$ ; the crosses also give those at the BKT point. The vertical arrow indicates the tricritical point. (c) The finite-size-scaling plot of  $\Delta E_\sigma$  at  $u = -1$ .

$z - z_2$  linearly couples to  $\varepsilon$ , we expect the plot with  $\nu = 1/(2 - x_\varepsilon) = \frac{5}{6}$  to yield a collapse of the finite-size data onto a single curve. The result exhibits a good scaling property and thus supports our prediction. On one hand, for  $u < -1.5$ , we find deviations of data from the values, which implies that the system is approaching the tricritical point. We search it along  $z_2(w)$ , using the criterion  $x_{3,3}^{(6)} = \frac{2}{21}$  [see Fig. 3(b)] [28] and estimate  $(w_t, z_t) \simeq (5.38, 5.03)$ , which is given by the open square in Fig. 2 (the monomer density is estimated as around 25%). To check its criticality, we estimate the central charge and scaling dimensions of the thermal operators. The results are  $c \simeq 0.859$ ,  $x_{1,2}^{(6)} \simeq 0.293$ , and  $x_{1,3}^{(6)} \simeq 1.439$ . We thus find reasonable agreement (within a few percent) between the numerical data and the theoretical predictions which strongly supports our RG argument.

In the strong-doping region, we have found some data to imply a first-order phase transition, e.g., an abrupt change in the monomer density and a double-peak structure in the monomer-density distribution function. These could be used as means to determine the phase transition boundary  $z_1(w)$ . However, we provide here numerical solutions of the PRG equation, represented by filled squares with the curve in Fig. 2 because they are known to give accurate estimations [29]. For large  $z$  and  $w$ , we can analytically estimate the phase boundary via an energy comparison between the complete columnar state and the dimer vacuum. For the honeycomb lattice case,  $z = w$ , which is given by the dotted line in Fig. 2. We observe that filled squares asymptotically converge to the line.

In conclusion, motivated by recent experiments on IPM, we have investigated the MDM system on the honeycomb lattice. We have provided the global RG flow diagram, which determines universality classes of phase transitions. Also, we have performed numerical calculations and provided evidence that supports our predictions. Regarding the relationship to experiment, there exist some issues. For instance, the phase diagram of

$\text{Dy}_2\text{Ti}_2\text{O}_7$  revealed a first-order phase transition between the kagome ice and the saturated state at  $H \simeq 0.9$  T for  $T < 0.36$  K [10]. In contrast, in our MDM system, the critical phase is not stabilized in the doped region. This implies that the long-range dipole interaction plays a crucial role for a stabilization of the kagome ice observed in real materials. However, this scenario is currently at the level of speculation, and its confirmation is left as a future work.

The author thanks K. Goto, H. Kadowaki, G. Tatara, M. Fujimoto, and K. Nomura for stimulating discussions. Main computations were performed by using the facilities at the Cyberscience Center in Tohoku University.

- 
- [1] R.H. Fowler and G.S. Rushbrooke, *Trans. Faraday Soc.* **33**, 1272 (1937).
  - [2] P.W. Kasteleyn, *Physica (Amsterdam)* **27**, 1209 (1961).
  - [3] H.N.V. Temperley and M.E. Fisher, *Phil. Mag.* **6**, 1061 (1961); M.E. Fisher, *Phys. Rev.* **124**, 1664 (1961).
  - [4] M.O. Blunt *et al.*, *Science* **322**, 1077 (2008).
  - [5] J.L. Jacobsen and F. Alet, *Phys. Rev. Lett.* **102**, 145702 (2009).
  - [6] H.W.J. Blöte and H.J. Hilhorst, *J. Phys. A: Math. Gen.* **15**, L631 (1982); B. Nienhuis, H.J. Hilhorst, and H.W.J. Blöte, *J. Phys. A: Math. Gen.* **17**, 3559 (1984).
  - [7] M.J. Harris *et al.*, *Phys. Rev. Lett.* **79**, 2554 (1997); A.P. Ramirez *et al.*, *Nature* **399**, 333 (1999).
  - [8] B.C. den Hertog and M.J.P. Gingras, *Phys. Rev. Lett.* **84**, 3430 (2000).
  - [9] K. Matsuhira *et al.*, *J. Phys.: Condens. Matter* **14**, L559 (2002); Z. Hiroi *et al.*, *J. Phys. Soc. Jpn.* **72**, 411 (2003).
  - [10] T. Sakakibara *et al.*, *Phys. Rev. Lett.* **90**, 207205 (2003).
  - [11] R. Moessner and S.L. Sondhi, *Phys. Rev. B* **63**, 224401 (2001); M. Udagawa, M. Ogata, and Z. Hiroi, *J. Phys. Soc. Jpn.* **71**, 2365 (2002).
  - [12] C. Castelnovo, R. Moessner, and S.L. Sondhi, *Nature* **451**, 42 (2008).
  - [13] S.T. Bramwell *et al.*, *Nature* **461**, 956 (2009); D.J.P. Morris *et al.*, *Science* **326**, 411 (2009); T. Fennell *et al.*, *Science* **326**, 415 (2009).
  - [14] H. Kadowaki *et al.*, *J. Phys. Soc. Jpn.* **78**, 103706 (2009).
  - [15] S.V. Isakov, K.S. Raman, R. Moessner, and S.L. Sondhi, *Phys. Rev. B* **70**, 104418 (2004).
  - [16] S.V. Isakov, R. Moessner, and S.L. Sondhi, *Phys. Rev. Lett.* **95**, 217201 (2005); for the kagome ice, see also Y. Tabata *et al.*, *ibid.* **97**, 257205 (2006).
  - [17] F. Alet *et al.*, *Phys. Rev. Lett.* **94**, 235702 (2005).
  - [18] S. Papanikolaou, E. Luijten, and E. Fradkin, *Phys. Rev. B* **76**, 134514 (2007).
  - [19] C.L. Henley, *J. Stat. Phys.* **89**, 483 (1997).
  - [20] H. Otsuka, *Phys. Rev. E* **80**, 011140 (2009).
  - [21] P. Lecheminant, A.O. Gogolin, and A.A. Nersisyan, *Nucl. Phys. B* **639**, 502 (2002).
  - [22] A.B. Zamolodchikov, *Sov. J. Nucl. Phys.* **46**, 1090 (1987).
  - [23] A.W.W. Ludwig and J.L. Cardy, *Nucl. Phys. B* **285**, 687 (1987).
  - [24] B. Nienhuis, *J. Phys. A: Math. Gen.* **15**, 199 (1982).
  - [25] J.L. Cardy, *J. Phys. A: Math. Gen.* **17**, L385 (1984).
  - [26] H.W.J. Blöte, J.L. Cardy, and M.P. Nightingale, *Phys.*

- Rev. Lett. **56**, 742 (1986); I. Affleck, *ibid.* **56**, 746 (1986).
- [27] B. Derrida and L.De. Seze, J. Phys. (Paris) **43**, 475 (1982).
- [28] X. Qian, Y. Deng, and H.W.J. Blöte, Phys. Rev. E **72**, 056132 (2005)
- [29] P.A. Rikvold *et al.*, Phys. Rev. B **28**, 2686 (1983); V. Privman and M.E. Fisher, J. Stat. Phys. **33**, 385 (1983).